A Humidity-Insensitive NO_2 Gas Sensor With High Selectivity

Xiaofang Pan, *Member, IEEE*, Xiaojin Zhao, *Member, IEEE*, Amine Bermak, *Fellow, IEEE*, and Zhiyong Fan, *Member, IEEE*

***Abstract*— Gas sensors based on semiconductor–metal–oxide nanomaterial have recently emerged due to their advantages of offering large surface to volume ratio. Unfortunately, these sensors are vulnerable to environmental humidity and lack of selectivity when exposed to common gases in air. In this letter, a novel morphology of ZnO nanomaterial is proposed for fabricating NO_2 gas sensor through our customized vapor trapping chemical vapor deposition process. By operating the fabricated gas sensors at the room temperature, high sensing performance, including a large output response of 11.06 and a short response/recovery time of 107/124 s, is achieved for 20-ppm NO_2. Moreover, the sensor response remains stable under humid environment up to 76%RH. In addition, the extensive experimental results indicate that our fabricated NO_2 gas sensors exhibit high selectivities of 61.7, 42.8, and 54.4 dB for different target gases of H_2, CH_2O, and C_6H_6, respectively. These features will enable the mass fabrication of miniaturized, cost-effective, and highly robust gas sensor suitable for real-life application.**

***Index Terms*— Semiconductor metal oxide nanomaterial, humidity-insensitive, high selectivity, room temperature, NO_2 gas sensor.**

I. Introduction

AS ONE of the primary air pollutants, NO_2 is toxic even at low concentrations, and the inhalation exposure is quite detrimental to human health [1]. This greatly motivates the real-time accurate field monitoring of the air's NO_2 level (typically ∼5ppm) [1], and various NO_2 gas sensor implementations have been demonstrated in the literature [2]. Among them, semiconductor metal oxide (SMO) nanomaterial-based gas sensors show great promise in terms of manufacturing cost [3], and more importantly, high sensing performance due to its inherent extremely large surface-to-volume ratio [4]. In [5], Yu *et al.* presented a tin dioxide nanobelt based gas sensor for measuring 0.2∼10ppm NO_2 at 200°C. In addition, a ZnO nanonail array was demonstrated to have a DC resistance change for 200ppm NO_2 at 225°C [6]. Moreover, Zhang *et al.* fabricated different nanoparticles and nanotubes using various materials: $CuCo_2O_4$, $NiCo_2O_4$ and $ZnCo_2O_4$. A maximum response of 0.72 for 400ppm NO_2 at 300°C was reported [2]. Despite the reported attractive sensing performance, the sensors' strong dependence on the environmental factors (e.g. humidity) significantly limits their application beyond laboratory environment [7]. In addition, with the existence of several common interfering gases having variable concentrations, such as the reducing gas of H_2 and the vapors of organic compound solvents (VOC) gases of CH_2O/C_6H_6, the NO_2 sensing results of the aforesaid implementations are not repeatable any more, showing very poor selectivity [8]. Furthermore, it is required to operate these sensors at a high temperature over 200°C, which requires a dedicated heating component and results in prohibitively higher power consumption [9]. This is a major limiting factor when the sensors are integrated into the mobile gas sensing devices with stringent power consumption budget.

In this letter, a versatile humidity-insensitive gas sensor based on a novel ZnO morphology, namely ZnO hierarchical nanostructure, is presented. Featuring high selectivity from different interfering gases, the proposed gas sensor exhibits superior sensing performance even at room temperature and shows long-term stability under various humid environments.

II. Device Fabrication

Ultrasonic-based methods, such as "drop-cast", are widely exploited for fabricating nanostructure based device. These processes, typically conducted in organic solution (e.g. IPA), cannot preserve the grown nanomaterial's fine morphology, leading to very poor yield and inferior device performance. Additionally, a time-consuming manual inspection is always needed in the following step to make sure reliable connections with the pre-fabricated metal pads are achieved. In this work, an "ultrasonic & solution-free" process flow is developed to grow our proposed ZnO hierarchical nanostructure. Specifically, as shown in Fig. 1, a finger-crossed triple-metal-layer

Manuscript received October 26, 2015; revised November 8, 2015; accepted November 19, 2015. Date of publication November 26, 2015; date of current version December 24, 2015. This work was supported in part by the Hong Kong Innovation and Technology Fund under Grant ITS/195/14FP, in part by the General Research Fund from the Hong Kong Research Grant Council under Grant 612113, in part by the National Natural Science Foundation of China under Grant 61504087, in part by the Kongque Technology Innovation Foundation of Shenzhen under Grant KQCX20120807153227588, and in part by the Fundamental Research Foundation of Shenzhen under Grant JCYJ20140418095735624 and Grant JCYJ20150324141711677. The review of this letter was arranged by Editor A. Flewitt.

X. Pan is with the College of Information Engineering, Shenzhen University, Shenzhen 518060, China, and also with the Department of Electronic and Computer Engineering, The Hong Kong University of Science and Technology, Hong Kong.

X. Zhao is with the College of Electronic Science and Technology, Shenzhen University, Shenzhen 518060, China (e-mail: eexjzhao@szu.edu.cn).

A. Bermak is with the College of Science and Engineering, Hamad Bin Khalifa University, Doha 5825, Qatar, and also with the Department of Electronic and Computer Engineering, The Hong Kong University of Science and Technology, Hong Kong.

Z. Fan is with the Department of Electronic and Computer Engineering, The Hong Kong University of Science and Technology, Hong Kong.

Color versions of one or more of the figures in this letter are available online at http://ieeexplore.ieee.org.

Digital Object Identifier 10.1109/LED.2015.2504260

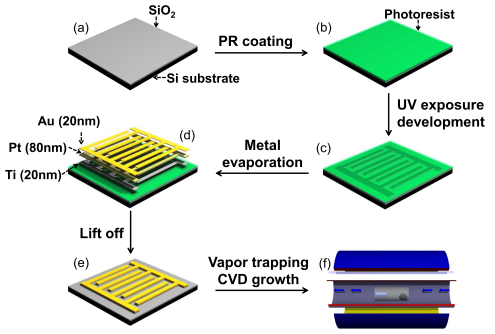

Fig. 1. Optimized fabrication process flow of our proposed ZnO nanomaterial based gas sensor. (a) clean Si wafer with 1 μm SiO_2; (b) photoresist coating; (c) photoresist exposure/patterning; (d) triple-layer metal evaporation; (e) photoresist lift-off; (f) hierarchical nanostructure growth by VTCVD process.

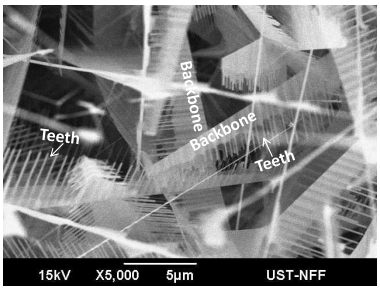

Fig. 2. The SEM picture of our fabricated ZnO hierarchical nanostructure.

structure (Au/Pt/Ti) is prepared with standard evaporation and lift-off methods (Fig. 1(a)-(e)). Successively, all the ZnO hierarchical nanostructures are directly grown on top of the patterned electrodes by our customized vapor trapping chemical vapor deposition (VTCVD) process (Fig. 1(f)) [10].

III. Results and Discussion

In this section, the fabricated ZnO hierarchical nanostructure is first examined using scanning electron microscope (SEM). In Fig. 2, it is observed that our proposed hierarchical nanostructure possesses a "comb" shape with parallel "teeth" connected to the "backbone". The electrode gap is measured to be 10μm and the thickness of the sensing layer is $\sim$15μm. Furthermore, temporal gas sensing measurement was conducted at the room temperature for NO_2 concentration ranging from 1ppm to 20ppm. Figure 3 presents the sensor's output response, which is defined as the measured relative resistance change after the exposure to NO_2 [i.e. $(R_{NO2}-R_o)/R_o$, where R_o is the original measured resistance]. The number of sensors tested is 6. The mean resistance of sensors is measured to be 20.6kΩ at room temperature, with a standard deviation of 3.28kΩ. In addition, the room temperature and the humidity for Fig. 3 are 25°C and 4%RH, respectively. All the gases including NO_2 and air were dehumidified before the test with a flow rate of 250sccm. Under all the different concentrations, our fabricated sensor shows consistent response/recovery curves for every two consecutive cycles with the same concentration, validating the sensor's superior repeatability and stability. In particular, we conducted an additional different test for 1ppm NO_2: a step change of NO_2

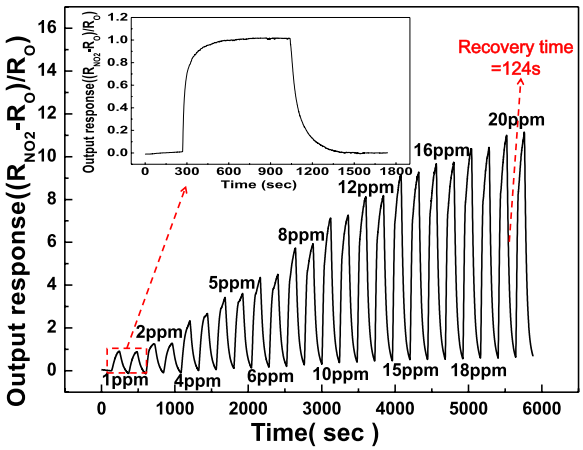

Fig. 3. The measured temporal output response of our fabricated gas sensor for 1ppm$\sim$20ppm NO_2.

concentration from 0ppm to 1ppm is adopted to demonstrate the response time in the inset of Fig. 3. As a result, it takes 345 seconds for the fabricated sensor to reach the full saturation (i.e. peak output response of 1.0). Here the response time is defined as the time interval of the measured output response increasing to 90% of the difference between the peak output response and the baseline, therefore, the response time is measured to be 110 seconds. When the concentration increases to 20ppm, the output response rises up to 11.06 with a response/recovery time of 107s/124s. Here the full saturation of 20ppm NO_2 was not achieved and we chose not to report the peak output response of 20ppm NO_2 for trading-off the measured response/recovery time. Additionally, we would like to point out that: compared with the state-of-the-art output response of SMO-based implementations for NO_2 gas (i.e. 0.8, measured at 200°C for 10ppm NO_2) [5], the output response of our fabricated gas sensor (i.e. 7.26, 10ppm in Fig. 3), even measured at the room temperature and without saturation, greatly outperforms, which is explicitly attributed to the dramatically elevated surface-to-volume ratio of our proposed ZnO "nanocomb" morphology and its unique electron transport mechanism [11]. Concretely, resulted from the surface trap states, the equivalent energy band is bent at the ZnO nanostructure's surface. When two or more nanostructures are connected, an energy barrier can be formed at each intersection point. Its influences on the transport of the electrons can be quantitatively expressed as follows:

$$G = G_0 \exp(-\phi^{eff}/k_B T) \quad (1)$$

where ϕ^{eff} denotes the effective barrier height, k_B is the Boltzmann's constant, T is the absolute temperature and G is the conductance of the intersection point. In this equation, G_0 can be considered as a constant parameter. Typically, when exposed to NO_2, ϕ^{eff} is increased owning to the electrons trapped by the adsorbed oxygen molecules of NO_2. Therefore, the conductance G decreases exponentially with the increment of the energy barrier height. This leads to an efficient conducting path manipulation by the numerous energy barriers, which corresponds to a large number of the aforesaid nanostructure connections.

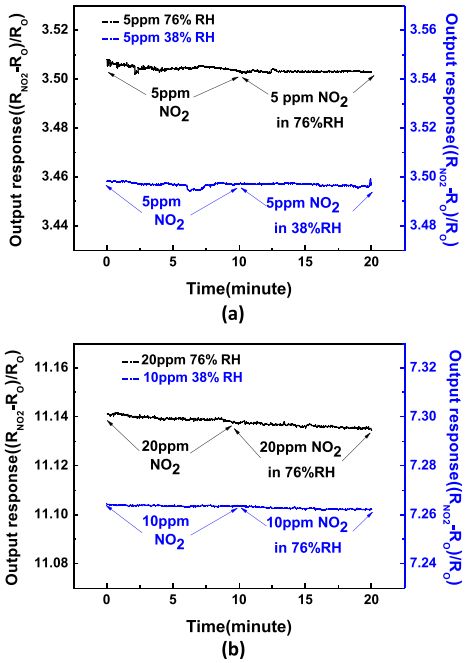

Fig. 4. The measured output response under different humid environments: (a) 5ppm at 38%RH and 76%RH environment; (b) 10ppm and 20ppm at 76%RH environment.

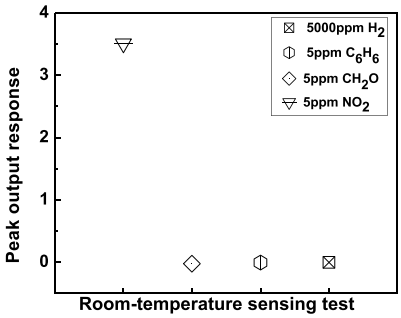

Fig. 5. The fabricated gas sensor's mean peak output responses for NO_2 and three different interfering gases: H_2, CH_2O and C_6H_6.

In order to mimic the gas sensors' real application environment with variable humidities, we conducted the temporal output response measurement under different humidities. In Fig. 4, the measured output response shows extremely weak influence by the injected humid air with both humidities of 38%RH and 76%RH. Compared with most previously reported implementations vulnerable to variable humidities [12], [13], our proposed gas sensors take great advantages in terms of reliability and robustness, which enables the gas sensors' long-time application in real environment. In addition, the characterization of our fabricated ZnO hierarchical nanostructure is further extended to several common interfering gases: the reducing gas (H_2) and two typical VOC gases including CH_2O and C_6H_6. As illustrated in Fig. 5, for H_2, output response is not remarkable at the room temperature; meanwhile, there is no obvious output response observed for both aforesaid VOC gases at the room temperature. Here we define the selectivity as the decibel ratio of our sensor's NO_2 output response to the output responses of H_2, C_6H_6 and CH_2O, respectively. As a result, according to Fig. 5, our NO_2 gas sensor's selectivities to H_2, CH_2O and C_6H_6 are calculated to be 61.7dB, 42.8dB and 54.4dB, respectively. Table I further summarizes the peak output response comparison of NO_2 and the aforesaid three different interfering gases. Compared with the previously reported polymer based implementations [12], [13], our proposed NO_2 gas sensor, featuring superior selectivity, takes significant advantages. In order to explain our fabricated sensor's superior selectivity, we would like to point out that NO_2, H_2, C_6H_6 and CH_2O are differently categorized, resulting from their various responses to standard semiconductor metal oxide (SMO) materials (e.g. ZnO). Concretely, H_2, C_6H_6 and CH_2O are typically regarded as the reducing gas, which can decrease the SMO materials' resistance [14]–[16]. However, for NO_2, it is typically categorized as oxidizing gas [17], which tends to increase the resistance of SMO materials.

TABLE I

PEAK OUTPUT RESPONSE COMPARISON OF NO_2 AND THREE DIFFERENT INTERFERING GASES

	NO_2 5ppm	H_2 5000ppm	CH_2O 5ppm	C_6H_6 5ppm
Mean	3.51	0.00289	0.02552	0.00667
Standard Deviation (SD)	0.127	0.00109	0.011	0.00763
Selectivity (dB)	N/A	61.7	42.8	54.4

Regarding the repeatability of the experimental results, we would like to state that the same samples were intensively measured, with a time interval of 12 months between the first and the most recent measurements. More importantly, for each time of intensive measurement, the same samples had to go through different continuous tests for hours, even days, including the tests of temporal response, humidity-dependence and selectivity, etc. As a result, we have not observed any significant performance deviation of our fabricated ZnO nanostructures. Moreover, it is worthy to mention that the gas sensing is quite application-specific and here in this work, we mainly target on the indoor NO_2 gas sensing applications with selected interfering gases of H_2, CH_2O, C_6H_6. Efforts are still ongoing for characterizing the other common interfering gases (e.g. O_3).

IV. CONCLUSIONS

We present a VTCVD-based direct-growth recipe for fabricating ZnO hierarchical nanostructure on top of patterned electrodes of silicon chip. Attributing to the demonstrated unique "nanocomb" morphology, room-temperature peak responses of 0.9 and 11.06 are reported for 1 ppm and 20 ppm NO_2, respectively, with the measured response/recovery time of ~2 min. In addition, our fabricated NO_2 sensor features humidity-insensitive and exhibits high selectivities to several common interfering gases widely existing in the environment, which paves the way to mass production of gas sensors development in real-life application.

REFERENCES

[1] N. D. Hoa and S. A. El-Safty, "Synthesis of mesoporous NiO nanosheets for the detection of toxic NO_2 gas," *Chem.-Eur. J.*, vol. 17, no. 46, pp. 12896–12901, 2011.

[2] G.-Y. Zhang, B. Guo, and J. Chen, "MCo_2O_4 (M = Ni, Cu, Zn) nanotubes: Template synthesis and application in gas sensors," *Sens. Actuators B, Chem.*, vol. 114, no. 1, pp. 402–409, 2006.

[3] E. Comini, G. Faglia, G. Sberveglieri, Z. Pan, and Z. L. Wang, "Stable and highly sensitive gas sensors based on semiconducting oxide nanobelts," *Appl. Phys. Lett.*, vol. 81, no. 10, pp. 1869–1871, 2002.

[4] B. Wang, L. F. Zhu, Y. H. Yang, N. S. Xu, and G. W. Yang, "Fabrication of a SnO_2 nanowire gas sensor and sensor performance for hydrogen," *J. Phys. Chem. C*, vol. 112, no. 17, pp. 6643–6647, 2008.

[5] C. Yu, Q. Hao, S. Saha, L. Shi, X. Kong, and Z. L. Wang, "Integration of metal oxide nanobelts with microsystems for nerve agent detection," *Appl. Phys. Lett.*, vol. 86, no. 6, p. 063101, 2005.

[6] S. Kar, B. N. Pal, S. Chaudhuri, and D. Chakravorty, "One-dimensional ZnO nanostructure arrays: Synthesis and characterization," *J. Phys. Chem. B*, vol. 110, no. 10, pp. 4605–4611, 2006.

[7] G. Korotcenkov, I. Blinov, V. Brinzari, and J. R. Stetter, "Effect of air humidity on gas response of SnO_2 thin film ozone sensors," *Sens. Actuators B, Chem.*, vol. 122, no. 2, pp. 519–526, 2007.

[8] H. Xu, X. Liu, D. Cui, M. Li, and M. Jiang, "A novel method for improving the performance of ZnO gas sensors," *Sens. Actuators B, Chem.*, vol. 114, no. 1, pp. 301–307, 2006.

[9] J. W. Gardner, P. K. Guha, F. Udrea, and J. A. Covington, "CMOS interfacing for integrated gas sensors: A review," *IEEE Sensors J.*, vol. 10, no. 12, pp. 1833–1848, Dec. 2010.

[10] P.-C. Chang, Z. Fan, D. Wang, W.-Y. Tseng, W.-A. Chiou, J. Hong, and J. G. Lu, "ZnO nanowires synthesized by vapor trapping CVD method," *Chem. Mater.*, vol. 16, no. 24, pp. 5133–5137, 2004.

[11] X. Pan, X. Zhao, J. Chen, A. Bermak, and Z. Fan, "A fast-response/recovery ZnO hierarchical nanostructure based gas sensor with ultra-high room-temperature output response," *Sens. Actuators B, Chem.*, vol. 206, pp. 764–771, Jan. 2015.

[12] M. Hübner, C. E. Simion, A. Tomescu-Stănoiu, S. Pokhrel, N. Bârsan, and U. Weimar, "Influence of humidity on CO sensing with p-type CuO thick film gas sensors," *Sens. Actuators B, Chem.*, vol. 153, no. 2, pp. 347–353, 2011.

[13] H.-R. Kim, A. Haensch, I.-D. Kim, N. Barsan, U. Weimar, and J.-H. Lee, "The role of NiO doping in reducing the impact of humidity on the performance of SnO_2-based gas sensors: Synthesis strategies, and phenomenological and spectroscopic studies," *Adv. Funct. Mater.*, vol. 21, no. 23, pp. 4456–4463, 2011.

[14] C. Xiangfeng, J. Dongli, G. Yu, and Z. Chenmou, "Ethanol gas sensor based on $CoFe_2O_4$ nano-crystallines prepared by hydrothermal method," *Sens. Actuators B, Chem.*, vol. 120, no. 1, pp. 177–181, 2006.

[15] C.-Y. Lee, C.-M. Chiang, Y.-H. Wang, and R.-H. Ma, "A self-heating gas sensor with integrated NiO thin-film for formaldehyde detection," *Sens. Actuators B, Chem.*, vol. 122, no. 2, pp. 503–510, 2007.

[16] J. X. Wang, X. W. Sun, Y. Yang, H. Huang, Y. C. Lee, O. K. Tan, and L. Vayssieres, "Hydrothermally grown oriented ZnO nanorod arrays for gas sensing applications," *Nanotechnology*, vol. 17, no. 19, pp. 4995–4998, 2006.

[17] M.-W. Ahn, K.-S. Park, J.-H. Heo, J.-G. Park, D.-W. Kim, K. J. Choi, J.-H. Lee, and S.-H. Hong, "Gas sensing properties of defect-controlled ZnO-nanowire gas sensor," *Appl. Phys. Lett.*, vol. 93, no. 26, p. 263103, 2008.